Representing uncertainty in climate change scenarios: a Monte-Carlo approach

Mark New [a] and Mike Hulme [b]

[a] *School of Geography and the Environment, University of Oxford, Mansfield Road, Oxford OX1 3TB, UK*
[b] *Climatic Research Unit, School of Environmental Sciences, University of East Anglia, Norwich NR4 7TJ, UK*

Climate change impact assessment is subject to a range of uncertainties due to both incomplete and unknowable knowledge. This paper presents an approach to quantifying some of these uncertainties within a probabilistic framework. A hierarchical impact model is developed that addresses uncertainty about future greenhouse gas emissions, the climate sensitivity, and limitations and unpredictability in general circulation models. The hierarchical model is used in Bayesian Monte-Carlo simulations to define *posterior* probability distributions for changes in seasonal-mean temperature and precipitation over the United Kingdom that are conditional on *prior* distributions for the model parameters. The application of this approach to an impact model is demonstrated using a hydrological example.

1. Introduction

The assessment of impacts of future anthropogenic climate change on environmental and socio-economic systems is subject to a range of uncertainties, due to either "incomplete" knowledge or "unknowable" knowledge [1] (other typologies of uncertainty are possible – see Schneider et al. [2] for a recent review). Incomplete knowledge, which can potentially be redressed in future, arises from inadequate information or understanding about biophysical processes or a lack of analytical resources available for impact assessment. Examples include poorly understood climate physics and computing limitations, both of which limit the accuracy of general circulation model (GCM) climate change simulations. Unknowable knowledge stems from the inherent unpredictability of the Earth system and from our inability to forecast future socio-economic and human behaviour in a deterministic manner. An example of this type of unpredictability arises due to natural climate variability, both in the real world and in model simulations [3]. Uncertainties about future socio-economic trends have resulted in the wide range of future greenhouse gas (GHG) emissions pathways reported in the literature [4,5]. These unknowables are not "wholly unknowable" because there are formal procedures that can be used to define subjective or relative probabilities of occurrence – without knowing the exact probability of a particular event, we can still tell whether it is likely or unlikely.

These uncertainties (arising from incomplete and unknowable information) cascade through any climate change impacts assessment in an inter-dependent, but not necessarily additive or multiplicative, manner [6] (figure 1). The uncertainty surrounding future emissions is further compounded when attempts are made to translate emissions scenarios into atmospheric concentrations because of incomplete knowledge about sources and sinks of GHGs and

about their rates of recycling in the Earth system. When GHG concentrations are then used to drive GCMs in transient climate change simulations, a plethora of additional uncertainties arise from the structural/computational limitations and deficiencies in the physics of the GCMs [7]. Uncertainties in the representation of the mean state and variability of observed climate [8] will affect both the evaluation of GCM results and the development and evaluation of climate impact models. Finally, outputs from impact models are subject to uncertainties resulting from unknown aspects of the physics, biology and/or sociology of the system being simulated, from inadequacies in the model de-
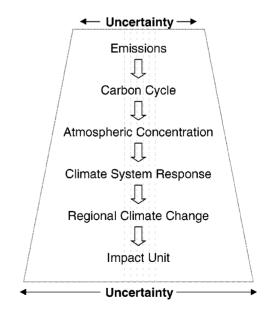

Figure 1. Schematic showing some of the uncertainties that cascade through a climate change impacts assessment. The total uncertainty (illustrated by the grey panel, but not to scale) expands as individual uncertainties are combined.

sign, and from an inability to predict how the system might adapt to changing climatic conditions (with or without deliberate human intervention).

Climate change impacts assessments have typically addressed these uncertainties in a limited and often haphazard manner, either through the use of scenarios, or through sensitivity studies, or through a combination of the two [9,10]. Using a single climate change scenario for an impact study represents a top-down approach to the problem and defines a single trajectory through the cascade of uncertainties described above. No quantified probability is attached to the simulated outcome. This approach is not particularly useful for risk and adaptation studies. Using several climate change scenarios provides the end-user of the impact study with a range of possible outcomes, but again with no attached probabilities. Sensitivity studies are typically bottom-up in approach, in that the sensitivity of an impact system to a range of future incremental climate perturbations is assessed. This is usually achieved using an impact simulation model. A sensitivity study can identify response thresholds in the modelled system and contribute towards defining a "dangerous" climate change space for the impact unit [11]. Such studies have not generally assessed the sensitivity of outputs to uncertainties inherent to the impact model (e.g., uncertain parameter values), but have instead focussed on the sensitivity to different climate inputs [12].

This study demonstrates one attempt to quantify some of the uncertainties associated with climate change impacts assessments using a Bayesian Monte-Carlo analysis of GHG emissions and climate model results. We use the United Kingdom as our example. Section 2 describes the Monte-Carlo methodology and the various input data sets and/or models used. This is followed in section 3 by a description of our results, including an assessment of the relative magnitude of each source of uncertainty addressed by our method. We give an example in section 4 of how our randomised climate change scenarios can be applied to a particular impact model, in this case a hydrological example. We conclude in section 5 with a discussion of the merits of this approach and the implications for climate change impact and adaptation research and for climate system modelling.

2. Methodology

A Bayesian Monte-Carlo approach to decision-making involves: (a) the definition of prior probabilities for the parameters of the model in question; (b) multiple simulations of the outcome(s) of the model by randomly sampling the parameter space according to the pre-defined probability distributions; and (c) the definition of the posterior probability (or frequency) distribution of the outcomes [12,13].

We define a multi-level model that samples several greenhouse gas emissions scenarios, a range of climate sensitivities (a key GCM characteristic), and the results from fourteen transient climate change simulations made using GCMs. Each of these inputs is described in turn. This approach derives from that used by Jones [14], although we develop the sampling of GCM patterns to a greater degree and consider a wider range of uncertainties.

2.1. Greenhouse gas (GHG) emissions scenarios

Future emissions of GHGs and aerosols fall into the category of "unknowable" knowledge because they will be a function of inherently unpredictable socio-economic and technological behaviour (although we can make subjective judgements about what emissions have low or high probability – for example, 400 Gt CO_2 emissions can be ruled out except at extremely low probabilities). In an attempt to embrace this uncertainty, emissions modellers have adopted a scenario approach, whereby different assumptions are made about key emissions drivers such as population, economic growth and energy technology. Thus six emissions scenarios were published in the 1992 Intergovernmental Panel on Climate Change (IPCC) report (IS92a–f [5]) and more recently, the IPCC special report on emissions scenarios (SRES) [15] have prepared a set of 40 emissions scenarios. The latter set of SRES scenarios derives from four independent socio-economic storylines. Scenarios from any one storyline, however, can have markedly different emissions outcomes due to alternative interpretations of the storyline and due to differences between emissions models that quantify the impact of the socio-economic assumptions. In this process modellers have made subjective judgements in defining the storylines, about the structure of their models, and about what the parameter values of these models should be. The resultant emissions scenarios therefore contain an "in-built" subjectivity that precludes low-probability (in the opinion of the modellers) emissions futures.

We make use of the four preliminary SRES marker scenarios – A1, A2, B1 and B2 – considered to be most representative of each storyline [16]. These four scenarios encompass a large proportion (about 80–90%) of the range of emissions futures contained in both the SRES and in other emissions scenarios published in the wider literature (figure 2). We initially assume that each of these four emissions trajectories are equally likely to occur, although we later vary this assumption.

2.2. The climate sensitivity

We use the MAGICC climate model [17,18] to convert the emissions scenarios into atmospheric concentrations of the various greenhouse gases and hence to calculate global-mean temperature at three future 30-year time horizons centred on 2025 (the 2020s), 2055 (the 2050s) and 2085 (the 2080s).

MAGICC parameterises a number of key atmospheric and ocean processes allowing the model to emulate the behaviour of more complex GCMs. The strength of the terrestrial carbon sink and the oceanic deep-water formation rate are two of these key parameters, but in our ex-
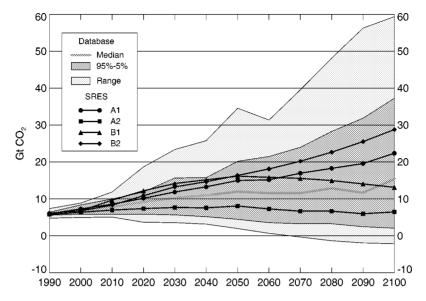
Figure 2. Preliminary SRES marker CO_2 emission scenarios [14] in the context of scenarios for CO_2 emissions from the wider literature (the "database") (A. Grübler, personal communication).

ercise we only consider the single most important parameter, the climate sensitivity. The climate sensitivity of the climate system can be defined as the increase in the equilibrium global-mean surface air temperature due to a doubling of atmospheric CO_2 concentration. The IPCC have always quoted the climate sensitivity to be in the range 1.5–4.5 °C [19,20]. In a study in which 16 leading climate scientists in the USA were asked to assign confidence intervals for the climate sensitivity [21], the majority of respondents put the lower 5th percentile at 1–2 °C and the upper 95th percentile at 4–7°C; this broadly corresponds to the IPCC range, but with a distribution skewed towards slightly higher temperatures. We adopt the IPCC range for the climate sensitivity parameter in our model and assume a simple triangular probability distribution (figure 3), implying that the central value of 3.0 °C is most likely. Other distributions are also possible. For example, Tol and De Vos [22], in a Bayesian analysis of expert opinion on the climate sensitivity showed that, with their model, the *posterior* distribution of the climate sensitivity was skewed towards higher values than the IPCC estimate. In contrast, Dickinson [23] has suggested a distribution skewed toward lower sensitivities, consistent with an analysis of uncertainties in climate feedbacks. We later assess the effect of alternative prior distributions of the climate sensitivity on the final outcomes of our hierarchical model.

We use MAGICC to calculate the global-mean temperature change at each time slice and under each emissions scenario, for the above range of climate sensitivities. Assuming (reasonably) that the probabilities of the four emissions trajectories and those of the climate sensitivity are independent, the resulting global-mean temperature outcomes may represent about 80% of the likely output distribution. Sulphate aerosol concentrations are not considered in our experimental design (although MAGICC can account for
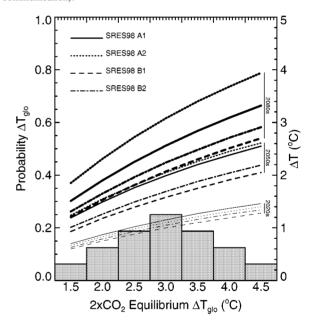

Figure 3. Global-mean temperature predicted by MAGICC as a function of the four preliminary SRES marker scenarios, and a range of climate sensitivities (histogram), by the 2020s (thin curve), 2050s (medium curve) and the 2080s (thick curve). The height of the histogram corresponds to the climate sensitivity probability distribution that was used in the initial simulations.

aerosol forcing). This is primarily because the mechanisms of aerosol forcing on climate are much less certain, and hence much more difficult to simulate than greenhouse gas forcing (in both MAGICC and the GCMS whose results are used later). Furthermore, by the end of the next century, which is the period from which we extract the GCM data, the forcing from aerosols is likely to be small relative to greenhouse gas forcing. Figure 3 summarises the global-mean temperature outcomes under the assumptions described in this and the previous section. These discrete outcomes, and their associated probabilities, were

integrated to 0.1 °C intervals to provide a more continuous prior distribution of global-mean temperature.

2.3. GCM uncertainties

The above analysis generates a distribution of global-mean temperature changes. We are interested, however, in relating these to regional climate change outcomes, for example, for domains within the UK. To achieve this next goal we therefore use the results of seven GCMs archived and described at the IPCC Data Distribution Centre (DDC [24]) to address two additional sources of uncertainty about future regional climate change. These uncertainties arise from GCM limitations and from climate system unpredictability. The model simulations available to us include two ensembles of four simulations each made using the HadCM2 GCM, plus single simulations made by six other models: ECHAM4, CSIRO-Mk2b, CGCM1, CCSR-98 and NCAR-DOE (see table 1). All these simulations were driven by changes in GHG forcing, without consideration of the effect of sulphate aerosols. The two HadCM2 ensembles were forced from 1990 by the IS92a and IS92d scenarios [5], corresponding approximately to 1 and 0.5% compound annual increases in CO_2 equivalent atmospheric concentrations. The remaining six simulations were all forced by similar (IS92a) 1% per annum compounded increases in GHG concentrations. The fourteen simulations are treated as a "super-ensemble", in which differences in regional climate outcomes due to inter-model differences and climate system unpredictability are not differentiated.

Results from each simulation were given equal prior probability under the assumption that all models perform equally well. Although this will not be the case, it is a reasonable initial assumption to make. As a consequence, the HadCM2 GCM is sampled nearly 60% of the time (8/14). This implies that uncertainty due to inter-model differences is not sampled uniformly, but uncertainty due to system unpredictability is sampled uniformly.

Table 1

Characteristics of the seven GCMs available at the IPCC Data Distribution Centre from which experimental results were used in this study.[a]

	Country of origin	Approximate resolution (lat. × long.)	Climate sensitivity (°C)	Integration length	Reference
CCSR-98	Japan	5.62° by 5.62°	3.5	1890–2099	[35]
CGCM1	Canada	3.75° by 3.75°	3.5	1900–2100	[36]
CSIRO-Mk2	Australia	3.21° by 5.62°	4.3	1881–2100	[37]
ECHAM4	Germany	2.81° by 2.81°	2.6	1860–2099	[38]
GFDL-R15	USA	4.50° by 7.50°	3.7	1958–2057	[39]
HadCM2[b]	UK	2.50° by 3.75°	2.5	1860–2099	[40]
NCAR-DOE	USA	4.50° by 7.50°	4.6	1901–2036	[41]

[a] Only the greenhouse gas forced integrations were used here. The climate sensitivity describes the equilibrium global-mean surface air temperature change of each model following a doubling of atmospheric carbon dioxide concentration.

[b] Two ensembles of four climate change simulations each were available from the HadCM2 model.

We extracted climate change signals in mean temperature (ΔT) and precipitation (ΔP) for the 30-year period centred on the 2080s for winter (DJF) and summer (JJA) seasons from each simulation for model land grid boxes located over Scotland and Eastern England. The 2080s period was used to maximise the climate change signal-to-noise [25]. For the GFDL-R15 and NCAR-DOE simulations we used the period centred on the 2020s because the simulations only extend to 2057 and 2036, respectively. This difference in sampling period is accounted for by the pattern-scaling method described below.

To remove the effects of different GCM climate sensitivities, the varying GHG forcings that were used in each GCM run, and the contrasting time periods that were sampled, the regional climate change signal in each GCM was standardised against its respective global-mean temperature change for the sampled time period. These standardised results were then scaled by the global-mean temperature changes simulated by MAGICC using the output distribution created in section 2.2. In this way, the regional pattern of climate change by, say, the 2050s from a GCM with a large global warming by the 2080s (i.e., a high model climate sensitivity) would be scaled downwards in proportion to the ratio of the model's global warming to that computed by MAGICC in section 2.2. This pattern-scaling method was first proposed and illustrated by Santer et al. [26] and the technique has been widely adopted and developed further in other subsequent climate scenario studies (e.g., Schlesinger et al. [27]). It assumes that the regional *pattern* of climate change due to greenhouse gas forcing (the greenhouse "signal") remains invariant both over time and for different levels of forcing. There is some support in the literature for this contention (e.g., Mitchell et al. [25]), although Schneider and Thompson [28] have suggested that regional patterns of climate change may not be linearly related to the global temperature signal. The raw and standardised ΔT and ΔP signals are shown in figure 4.

Each GCM climate change signal represents one sample from the population of changes that would be produced by a suitably large ensemble of simulations using that particular GCM. The variance of this population would represent the unpredictability of the model climate system and should be similar to the variance of 30-year means simulated in the GCM control simulation. Some change in this 30-year multi-decadal variance may arise from GHG forcing, but we ignore this for now. We calculated the variance in 30-year mean seasonal temperature and precipitation for the respective grid boxes in the 1400-year HadCM2 control integration [29] and use these variances to add "climate system noise" to the extracted GCM ΔT and ΔP climate change signals. This is achieved by assuming a normal distribution for the forty six 30-year means extracted from the control integration and randomly sampling the standard deviates of this distribution. This random noise is then added as a final layer to our Monte-Carlo regional climate change outcomes. This approach is probably over-generous in its
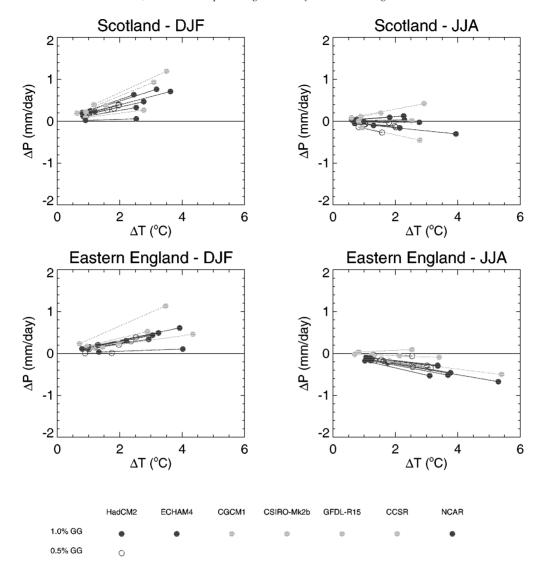
Figure 4. Pairs of scaled (left-hand symbols) and raw (right-hand symbols) 30-year mean changes (for the 2080s with respect to the 1961–1990 mean) in DJF and JJA mean temperature and precipitation over Scotland and Eastern England. The scaled changes are standardised against the corresponding GCM global-mean temperature change, and are therefore expressed in units of °C (or mm/day) per °C change in global-mean temperature. The raw changes were extracted directly from the GCMs for the 2080s period (except NCAR and GFDL where the 2020s were used). All GCM fields were interpolated onto the HadCM2 grid before the ΔT and ΔP information was extracted.

allowance for natural variability because the random noise is additive to the uncertainty about how far each individual GCM experiment result lies from the (infinitely large) ensemble or population mean.

3. Results

3.1. Initial simulations

Having defined a hierarchical probabilistic model to predict climate change in the 2080s over Scotland and Eastern England, we then ran an initial Monte-Carlo simulation of the model, with 50,000 iterations, using the *a priori* probability distributions described above. The outcomes, ΔT and ΔP in the 2080s, were a function of random sampling of emissions scenario, climate sensitivity, regional GCM signal and climate system noise, and were analysed to pro-

duce a two-dimensional posterior probability histogram for each region. The histogram was then contoured at the 95th, 75th, 50th, 75th and 5th percentiles (figure 5). The outermost contour therefore represents the 95th percentile, with 95% of all outcomes falling within this contour.

The basic shape of the *posterior* distribution is primarily controlled by the relatively small sample of GCM outputs. A large scatter in ΔP (as in Scotland in JJA) or ΔT (as in Eastern England in JJA) from the GCMs produces a correspondingly less compact posterior distribution. The climate noise component that was added ensures some negative DJF ΔP outcomes in both regions, despite none of the GCMs having a negative signal in this season. The relatively tightly constrained standardised ΔTs and ΔPs in Scotland (cf. figure 4) result in a similarly constrained 5th percentile in figure 4. The location of this central isoline is a function of the triangular *a priori* distribution assigned to
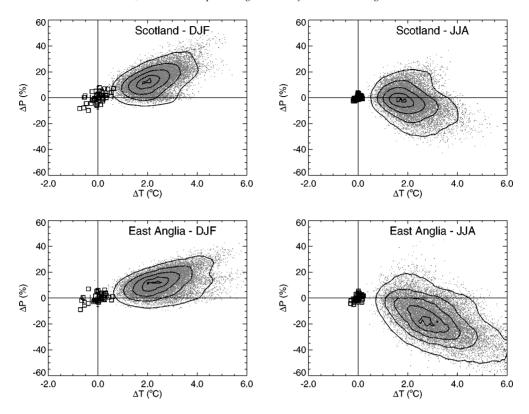
Figure 5. Results from the initial 50,000 Monte-Carlo simulations sampling the hierarchical model of ΔT and ΔP described in section 2. Dots represent individual outcomes of the model; contours are 95th, 75th, 50th, 25th and 5th percentiles of the resulting two-dimensional probability density histogram; squares are individual 30-year mean ΔT and ΔP over each region, calculated from the 1400 year HadCM2 control integration.

the climate sensitivity parameter. In contrast, the less compact distribution of GCM ΔTs and ΔPs for JJA in Eastern England (figure 4) results in a less compact *posterior* distribution (figure 5).

Also shown in figure 5 are 30-year means of T and P (expressed as anomalies from long-term mean) extracted from the 1400-year HadCM2 control integration, providing an indication of the natural variability (or climate noise) in mean seasonal temperature and precipitation that might be expected over the two regions. The entire range of future ΔT outcomes is clearly distinguishable from climate noise in the HadCM2 simulation, but only about half of the future winter ΔP outcomes (more in summer) are distinguishable from climate noise.

It is interesting to note that the positive correlations between ΔT and ΔP in winter in the control simulation for both regions are also present in the climate change outcomes, suggesting that this co-relationship is a fairly robust result in the future model world. The reasons for this are fairly well understood, with increased temperature resulting in a moister atmosphere (increased specific humidity) and consequent increased moisture flux into rainfall regions [30]. In contrast, the control simulation does *not* exhibit a strong T–P relationship in summer in either region. This result is paralleled by the climate change outcomes in Scotland, where the individual T–P changes in JJA do not display any marked correlation. In Eastern England, however, future JJA climates show a negative correlation between T and P. Mecha-

nisms driving these summer changes are not as well understood [30].

3.2. Other distributions

Our choice of *a priori* distributions for each parameter in the hierarchical model was rather arbitrary, with only the climate sensitivity assigned a non-uniform (non-diffuse) distribution. We investigated the sensitivity of the output distribution to alternative input distributions and found that, while the details of the posteriors varied, the overall pattern was similar to those described above. This is illustrated with a few examples in the sections that follow.

3.2.1. Individual models

We first investigated how the sampling of individual GCMs affects the results of the analysis. All input probability distributions, except for the GCMs, were kept the same as in the initial simulations. We sampled each GCM in turn in a series of separate Monte-Carlo simulations; thus, at each GCM iteration, the probability of the selected GCM was one and all others was zero. The results of this exercise for Scotland are displayed in figure 6. The different posterior distributions arise solely from the different ΔT and ΔP patterns of the GCMs (figure 4). Thus the CGCM1 posterior outcomes are the most tightly constrained because this GCM has the lowest ΔT and ΔP over the UK (when scaled by the model ΔT_{glo} climate sensitivity). The CCSR-98 and ECHAM4 posteriors are more elongate because these two
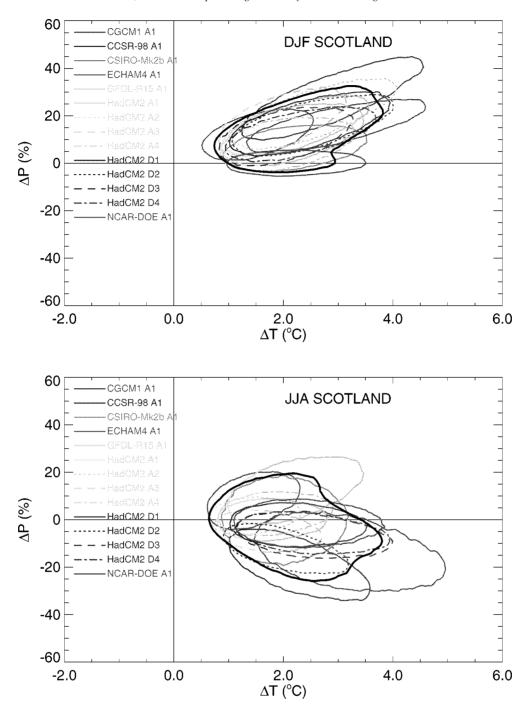
Figure 6. 95th percentiles of the outcomes of the hierarchical model over Scotland, when each GCM is sampled in turn. The bold black line is the 95th percentile of all model outcomes (i.e., assuming all models are equally likely). The model acronyms refer to the list in table 1; these are followed by "A" or "D", representing a 1% or 0.5% CO_2-equivalent forcing, and a number from one to four, representing the ensemble member number.

models have the largest scaled ΔTs. The combined posterior, using the results from all model outcomes, overlaps all the individual posteriors. Those outcomes that are different from the majority, however, do not have as great an overlap with the combined posterior (e.g., GFDL-R15 in JJA-Scotland). Clearly, if the set of simulations in section 3.1 was repeated assuming a non-uniform likelihood for the GCMs, the posteriors will be biased towards models with higher likelihood.

3.2.2. Climate sensitivity

In our initial simulations we assumed a triangular prior distribution for the climate sensitivity parameter. Here we investigate the sensitivity of the posterior to alternative priors for this parameter. A set of four simulations with different climate sensitivity priors was undertaken. As with previous simulations, the frequency distributions of climate sensitivity from 1.5 to 4.5 °C were expressed as simple integer values and re-expressed as a probability distribu-

Table 2
Frequency distributions of the climate sensitivity parameter used in each of four simulations to test the sensitivity of the model outcome distributions to the different *a priori* probability distribution of this parameter.

Simulation	Climate sensitivity/frequency						
	1.5 °C	2.0 °C	2.5 °C	3.0 °C	3.5 °C	4.0 °C	4.5 °C
1	1	5	8	3	1	1	0
2	1	0	0	0	0	0	0
3	1	0	0	0	0	0	1
4	1	2	3	4	3	2	1

tion that could be sampled on a Monte-Carlo basis. The prior distributions range in form from an extreme case, in which a single low sensitivity of 1.5 °C is sampled with a probability of 1.0, through bimodal and skewed triangular distributions, to the original symmetrical triangular shape used in section 3.1 (table 2).

The resulting posterior distributions vary as a function of the prior distributions, as illustrated for DJF East England (figure 7). The most elongate posterior arises from the bimodal (1000001) prior distribution, which maximises the sampling frequency at high and low climate sensitivities. As might be expected, the most constrained posterior is produced by the single-outcome (1000000) prior distribution, with the 95th percentile not extending beyond a ΔT of about 2.5 °C. The posteriors arising from the other two (triangular) priors are intermediate between these two end cases, and fairly similar.

The internal structure of the posterior distributions under these different sampling strategies for the climate sensitivity also differs. The triangular and skewed priors produce similar internal structures, as indicated by the 50th percentiles. The main difference lies in the symmetrical triangular prior producing a more elongate posterior. In contrast, the bimodal prior produces a similarly bimodal 50th percentile, and the single value prior results in a very tightly constrained 50th percentile.

3.2.3. SRES scenarios

In the initial set of simulations (section 3.1) we assumed that each preliminary SRES marker emissions scenario was equally likely. Figure 8 shows the effect of sampling each emissions scenario in isolation, once again for DJF over eastern England. In other words, we show the results of four separate Monte-Carlo simulations where one emissions scenario is in turn assigned a prior probability of one and the other three emissions priors are zero. All other parameters are sampled as in the initial exercise in section 3.1. By the 2020s there is little difference between the posteriors for each of these cases. This is because the emissions, and therefore the resulting global-mean temperatures, have not diverged very much from their common 1990 starting points, and also because a proportion of the warming is inherited from pre-1990s forcing, which was the same (i.e., that observed) in all scenarios.

By the 2080s, some larger differences between the SRES scenarios become apparent. Here the emissions, and hence the concentration pathways, have diverged more substantially as a consequence of different future worlds. Thus, it is only in the second half of the 21st century that different emissions futures begin to become distinguishable against the noise arising from other uncertainties in our model framework.

4. Application to an impact model

The approach described above provides one route to the quantification of uncertainty (or certainty) associated with regional climate change – expressed in terms of uncertainties in global-scale forcings and predictability, and in terms of the regional manifestations of global change. While this is a useful exercise in itself for providing a coherent framework for handling different sources of uncertainty in climate change scenarios, its full value becomes apparent when applied to an impact assessment [14]. Here we apply the results of a hydrological sensitivity analysis, where the response of river flow to changes in mean precipitation and temperature was simulated using a catchment hydrological model. The hydrological simulations enable the definition of a response surface of the hydrological variable of interest (in this case mean annual river flow) in climate change (ΔT and ΔP) space (figure 9, top).

The posterior probability distribution from the Monte-Carlo climate change analysis defined the likelihood of different ΔT and ΔP combinations over the hydrological response surface. This is also illustrated in figure 9 (top) where the joint posterior distribution of annual ΔT and ΔP for Scotland is overlaid on the hydrological response surface. The intersection of the posterior climate change distribution with the response surface therefore enabled the probability of annual flow at each point on the response surface to be defined in terms of the climate change probabilities arising from the Monte-Carlo simulations. The response surface could then be sampled in terms of the likelihood of changes in flow, expressed as a frequency distribution or, more usefully, a cumulative probability distribution for future flow (figure 9, middle).

Both the posterior climate change distribution that arises from the hierarchical model, and the derived probability distribution for the impact system of interest (in this case, annual river flow) represent a significant step towards a quantification of uncertainty, and therefore risk, that can be used by decision-makers [31]. The real power of this approach is illustrated in the bottom panel of figure 9. Here the calculation of the frequency distribution (and cumulative probability distribution) of changes in mean annual flow is repeated at twenty year intervals from 2000 to 2100. This enables the change in the probability of particular thresholds (which could be either "dangerous" or "desirable") to be tracked forward in time, and the identification of the time at which a user-defined probability of a
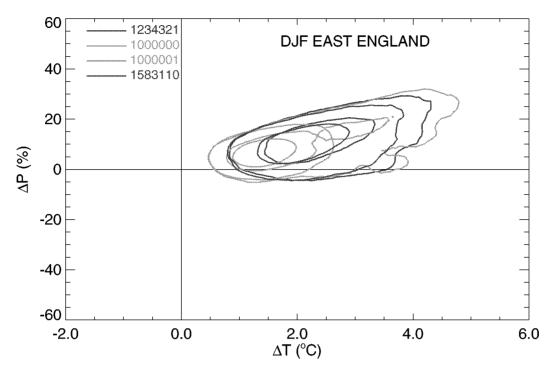
Figure 7. 95th and 50th percentiles of the posterior distributions for DJF East England, when different prior distributions for the climate sensitivity parameter are used (see section 3.2 and table 2 for details).
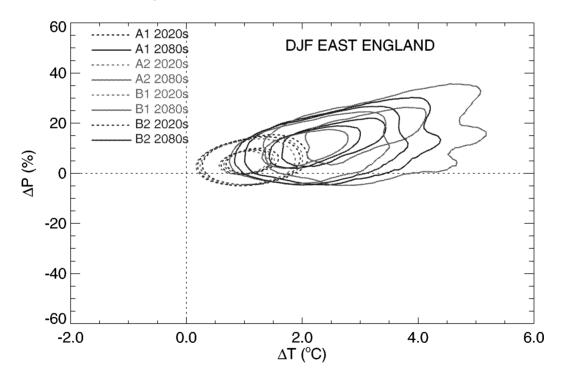

Figure 8. 95th and 50th percentiles of the posterior distributions for DJF East England, when each SRES emissions scenario is sampled in isolation, for different periods in the 21st century. Prior distributions of the other parameters remain as in the initial simulations in section 3.1.

threshold being exceeded is reached. For example, from figure 9 we can show that the probability of a 20% increase in mean annual flow expands from 0.05 in 2000 to 0.5 in 2100.

The approach used in this example makes no assumptions about parameter uncertainty in the hydrolog-

ical model. There is nothing preventing the integration of this hydrological model within our overall hierarchical Monte-Carlo model structure. With appropriate estimates for the hydrological model parameter prior distributions, a more comprehensive uncertainty analysis would be possible. Indeed, this approach to uncertainty
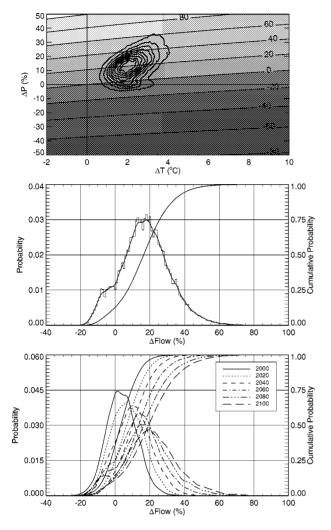
Figure 9. Application of the posterior probability distribution of the climate change model (Scotland annual) to a (nominal) response surface of change (in percent) in mean annual river flow in ΔT and ΔP space. Top: response surface showing the percent change in mean annual river flow as a function of ΔT and ΔP, with the posterior bivariate climate change frequency distribution superimposed on the response surface. Middle: the probability distribution and the cumulative probability distribution of changes in flow, derived by counting the relative frequency of the posterior climate change distribution at each point on the response surface (see section 4 for more detail). Bottom: the time-evolution of probabilities of changes in mean annual flow from 2000 to 2100.

analysis is already well established in hydrological modelling [32,33].

5. Discussion and conclusions

We have presented a methodology that quantifies a number of uncertainties inherent in the generation of future climate change information for climate impacts assessments. The approach is Bayesian in that it assumes that key parameters in our hierarchical predictive model have distributions that are either diffuse or defined. The model is then run in a Monte-Carlo simulation that samples the parameter space as defined by the prior probabilities. The model outputs – regional ΔT and ΔP – are then analysed to produce

an empirical bivariate probability distribution that can be used to quantify the uncertainty in the model predictions.

The model described here, however, represents an incomplete representation of uncertainties in climate change prediction. In particular, uncertainties in GCMs are only partially addressed by the use of a "super ensemble" of model outputs. The assumption here is that the range in GCM outputs is due to model inadequacies and parameter uncertainties, as well as due to climate system internal variability. A complete uncertainty analysis of GCM parameter values is theoretically possible [12], but beyond present day computing capacity. Even if such an analysis were feasible, uncertainty due to inadequacies in model physics would remain. In addition, the GCM results do not include outcomes that represent extremely low-probability high-impact events such as might be associated with the breakdown of the thermohaline circulation (THC) [34]. Most models do show a weakening of the THC, and its regional impact is therefore implicitly contained in the regional GCM patterns. A complete breakdown of the THC could conceivably be included in our model by introducing an arbitrary regional GCM response that yields cooling rather than warming, with an associated (subjective) probability distribution. Scaling the regional GCM changes in a negative direction may, however, be demanding too much of the pattern-scaling approach used here.

The four SRES emissions scenarios that were used represent a discrete (and incomplete) sample of the range of possible emissions futures. The full spectrum of SRES emissions futures encompasses 40 different scenarios and there are many additional scenarios in the refereed and popular literature. However, the four preliminary marker scenarios that we use span about 90% of the range in future emissions in the wider literature. If one assumes a diffuse prior probability for these scenarios (all equally likely), the posterior will be very similar to one where all 40 SRES emissions scenarios are sampled.

We have limited our analysis to a 21st century time frame. This clearly ignores the more "dangerous" climate changes that are likely to occur in the 22nd century and beyond, where tripling (or even quintupling) of CO_2 levels may occur. However, our main thrust has been to describe our methodology, not to define the evolving probabilities of particular thresholds for climate change over the United Kingdom. The examples we have used serve mainly to illustrate our approach.

As with the parameters in the GCMs, the hierarchical model used here does not address the full parameter uncertainty in the MAGICC climate model. These include assumptions about the rates of cycling, and sources and sinks, for CO_2 and other gases, and the conversion of atmospheric concentrations into global warming potentials. A more rigorous approach should also include these uncertainties.

We applied the model output probability distribution to a response surface of annual river flow in ΔT and ΔP space to derive a probability distribution for future flow changes

as a function of changes in the hydrological driving variables T and P. This "add on" approach to quantifying the effect of climate change on an impact system is an intermediate step towards a fully integrated modelling approach where the impact model is incorporated within the Bayesian Monte-Carlo framework. Full integration would enable an assessment of the influence of parameter uncertainty in the impact model on the final output distribution. This is work we intend to pursue in the future.

Acknowledgement

References

[1] M. Hulme and T.C. Carter, in: *Representing Uncertainty in Climate Change Scenarios and Impact Studies – ECLAT-2 Red Workshop Report*, eds. T. Carter, M. Hulme and D. Viner (Climatic Research Unit, Norwich, 1999).

[2] S.H. Schneider, W. Turner and H. Garriga-Morehouse, J. Risk. Res. 1 (1999) 165–185.

[3] F. Giorgi and R. Francisco, Clim. Dyn. 16 (2000) 169–182.

[4] J. Alcamo and N. Nakicenovic, Mitigation and Adaptation Strategies for Global Change (Special Issue) 3 (1998).

[5] J. Leggett et al., in: *Climate Change 1992: the Supplementary Report to the IPCC Scientific Assessment*, IPCC (Cambridge University Press, Cambridge, 1992).

[6] R.N. Jones, Clim. Change (2000), in press.

[7] W.L. Gates et al., Bull. Am. Meteor. Soc. 80 (1999) 29–55.

[8] M. New, in: *Representing Uncertainty in Climate Change Scenarios and Impact Studies – ECLAT-2 Red Workshop Report*, eds. T. Carter, M. Hulme and D. Viner (Climatic Research Unit, Norwich, 1999).

[9] T. Carter, M. Hulme and D. Viner, eds., *Representing Uncertainty in Climate Change Scenarios and Impact Studies – ECLAT-2 Red Workshop Report* (Climatic Research Unit, Norwich, 1999).

[10] M.L. Parry and T. Carter, *Climate Impact and Adaptation Assessment* (Earthscan, London, 1998).

[11] M. Hulme and O. Brown, Clim. Res. 10 (1998) 1–14.

[12] R.W. Katz, in: *Representing Uncertainty in Climate Change Scenarios and Impact Studies – ECLAT-2 Red Workshop Report*, eds. T. Carter, M. Hulme and D. Viner (Climatic Research Unit, Norwich, 1999).

[13] M.G. Morgan and M. Henrion, *Uncertainty: a Guide to Dealing with Uncertainty in Quamtitative Risk and Policy Analysis* (Cambridge University Press, Cambridge, 1990).

[14] R.N. Jones, Clim. Res. 14 (2000) 89–100.

[15] N. Nakicenovic, A. Grubler and A. McDonald, eds., Special report on emissions scenarios, Intergovernmental Panel on Climate Change (2000), in preparation.

[16] SRES, The Special Report on Emissions Scenarios (1999) (http://sres.ciesen.org).

[17] T.M.L. Wigley and S.C.B. Raper, Nature 357 (1992) 293–300.

[18] T.M.L. Wigley et al., MAGICC: Model for the Assessment of Greenhouse-Gas Induced Climate Change – Version 2.4 (Climatic Research Unit, Norwich, 2000).

[19] W.L. Gates et al., in: *Climate Change 1992: the IPCC Supplementary Report*, IPCC (Cambridge University Press, Cambridge, 1992).

[20] R.H. Moss and S.H. Schneider, Towards consistent assessment and reporting of uncertainties in IPCC TAR: initial recommendations for discussion by authors (1999), unpublished discussion document.

[21] M.G. Morgan and D.W. Keith, Environmental Science and Technology 29 (1995) A468–A476.

[22] R.S.J. Tol and A.F. De Vos, Clim. Change 38 (1998) 87–112.

[23] R.E. Dickinson, Adv. Geophys. 28 (1985) 99–129.

[24] IPCC-DDC, IPCC Data Distribution Centre GCM Scenario Download Website (1999) (http://ipcc-ddc.cru.uea.ac.uk/).

[25] J.F.B. Mitchell et al., Clim. Change 41 (1999) 547–581.

[26] B.D. Santer et al., Developing climate scenarios from equilibrium GCM results, report No. 218, Max-Planck Institute for Meteorology, Hamburg (1990).

[27] M.E. Schlesinger et al., Technological Forecasting and Social Change (2000), in press.

[28] S.H. Schneider and S.L. Thompson, J. Geophys. Res. 86 (1981) 3135–3147.

[29] S.F.B. Tett, T.C. Johns and J.F.B. Mitchell, Clim. Dyn. 13 (1997) 303–323.

[30] J.F.B. Mitchell et al., in: *Climate Change: the IPCC Scientific Assessment*, IPCC (Cambridge University Press, Cambridge, 1990).

[31] C. Green, R.J. Nicholls and C. Johnson, Climate Change Adaptation: an Analysis of Decision-Making in the Face of Risk and Uncertainty, report No. 28, NCRAOA (Environment Agency, 2000).

[32] K. Beven and A. Binley, Hydrol. Proc. 6 (1992) 279–298.

[33] J. Freer, K. Beven and B. Ambroise, Water Resour. Res. 32 (1996) 2161–2173.

[34] S. Rahmstorf and A. Ganopolski, J. Climate 12 (1999) 1349–1352.

[35] S. Emori et al., J. Meteorol. Soc. Jpn. (2000), submitted.

[36] G.J. Boer et al., Clim. Dyn. (2000), submitted.

[37] A.C. Hirst, S.P. Ofarrell and H.B. Gordon, J. Climate 13 (2000) 139–163.

[38] E. Roeckner et al., The Atmospheric General Circulation Model ECHAM-4: Model Description and Simulation of Present-Day Climate, report No. 218, Max-Planck Institute for Meteorology, Hamburg (1996).

[39] J.M. Haywood et al., Geophys. Res. Lett. 24 (1997) 1335–1338.

[40] J.F.B. Mitchell and T.C. Johns, J. Climate 10 (1997) 245–267.

[41] G.A. Meehl et al., J. Climate (2000), submitted.